Synthesis and Characterization of Polyurethane/Mg-Al Layered Double Hydroxide Nanocomposites

M. Kotal,[1] T. Kuila,[1] S. K. Srivastava,[1] A. K. Bhowmick[2]

[1]*Inorganic Materials and Nanocomposite Laboratory, Department of Chemistry, Indian Institute of Technology, Kharagpur 721302, India*
[2]*Rubber Technology Centre, Indian Institute of Technology, Kharagpur 721302, India*

Received 29 July 2008; accepted 7 March 2009
DOI 10.1002/app.30791
Published online 16 July 2009 in Wiley InterScience (www.interscience.wiley.com).

ABSTRACT: Layered double hydroxide (LDH) is a new type of nanofiller, which improves the physicochemical properties of the polymer matrix. In this study, 1, 3, 5, and 8 wt % of dodecyl sulfate-intercalated LDH (DS-LDH) has been used as nanofiller to prepare a series of thermoplastic polyurethane (PU) nanocomposites by solution intercalation method. PU/DS-LDH composites so formed have been characterized by X-ray diffraction and transmission electron microscopy analysis which show that the DS-LDH layers are exfoliated at lower filler (1 and 3 wt %) loading followed by intercalation at higher filler (8 wt %) loading. Mechanical properties of the nanocomposite with 3 wt % of DS-LDH content shows 67% improvement in tensile strength compared to pristine PU, which has been correlated in terms of fracture behavior of the nanocomposites using scanning electron microscope analysis. Thermogravimetric analysis shows that the thermal stability of the nanocomposite with 3 wt % DS-LDH content is $\approx$ 29°C higher than neat PU. Limiting oxygen index of the nanocomposites is also improved from 19 to 23% in neat PU and PU/8 wt% DS-LDH nanocomposites, respectively. J Appl Polym Sci 114: 2691–2699, 2009

Key words: polyurethanes; nanocomposites; mechanical properties; TGA; morphology

INTRODUCTION

Polymer nanocomposites derived from the two components, polymers and inorganic materials as fillers, have attracted a great interest for researchers because of their unexpected synergistical properties.[1] In polymer nanocomposites, the inorganic phase are in nanodimensional range.[2] The inorganic materials in nanometer range (nanofillers) generally used for the nanocomposite preparation contain silicate clay minerals,[3–8] manganese dioxide,[9] molybdenum sulfide,[10] layered phosphate,[11] layered double hydroxides (LDHs), etc.[12–19] Polymer nanocomposites are characterized by improved mechanical, thermal and barrier properties, reduced gas permeability, and flame retardancy in contrast to either the neat matrix or the conventional composites.[20–23] Such an improvement in properties of the nanocomposites is attributed to their unique phase morphology that maximizes the interfacial interaction between the well-dispersed nanometer size domains and the matrices. So far, most of the research works focus on polymer nanocomposites containing layered clays of natural origin, e.g., montmorillonite type of layered silicate compounds.[2,24–30] Recently, LDH has received more attention mostly due to their varieties of applications, e.g., catalysis, stabilizer, flame retardant materials, medical materials, adsorbents, ion-exchangers, and in environmental chemistry.[31] The novelty of LDHs with respect to other available nanofillers, e.g., sodium montmorillonite, hectorite provides a great flexibility in selecting organic modifiers (with respect to functional groups, such as carboxylates, sulfonates, phosphates, etc.) and various methods of modification process (such as *in situ* synthesis, ion-exchange, regeneration methods, etc.) and also its versatility in chemical compositions as well as multiple interaction with polymer.[17] In addition to the endothermic decomposition of the metal hydroxide layers, LDHs are often considered beneficial in improving the flame-retardancy of polymer nanocomposites.[17] Also in contrast to cationic clay mineral with negatively charged layers (1 : 1 or 2 : 1 type), the LDHs are a class of synthetic two-dimensional nanostructured anionic clays containing 1 : 1 brucite like layers, where a fraction of the divalent cations are coordinated octahedrally by hydroxyl groups and have been replaced isomorphously by trivalent cations giving positively charged layers.

Correspondence to: S. K. Srivastava (sunit@chem.iitkgp.ernet.in).

Contract grant sponsors: CSIR (New Delhi), DRDO (New Delhi).

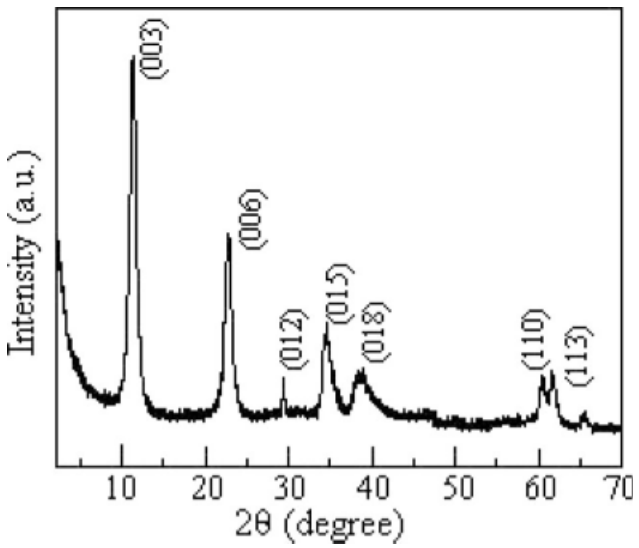

Figure 1 XRD pattern of pure Mg-Al LDH.

This positively charged interlayer space is occupied by some charge balancing anions to give neutral layered structure.[32,33] The pristine LDH is symbolized by the ideal formula $[M^{II}_{(1-x)}M^{III}_{x}(OH)_2]^{x+}A^{m-}_{x/m}\cdot nH_2O$, where M^{II} is a divalent metal cation, e.g., Mg^{2+}, Zn^{2+}, etc., M^{III} is a trivalent metal cation, e.g., Al^{3+}, Cr^{3+}, etc., and A is exchangeable interlayer anion with valancy *m* (like Cl^-, CO_3^{2-}, NO_3^-, etc). In pure inorganic LDH, the hydroxide sheets stacked with strong interaction due to high intergallery charge density, resulting in short interlayer spacing between the metal hydroxide layers (0.78 nm) making it not suitable for long polymer chain intercalation[18] which is shown in Figure 1. Hence, LDH is organomodified to increase the interlayer spacing by incorporating long chain organic anion. This, in turn, facilitates the penetration of the larger polymer chains within this interlayer spacing making it more compatible with the organic polymer.[12–19,34,35]

Polymer/LDH nanocomposites are reported to be synthesized by *in situ* polymerization, direct intercalation, coprecipitation, and restacking of LDH in polymer solution.[29–31] Earlier studies[18,34,35] have shown that solution intercalation is one of the best preparative methods to synthesize polymer/LDH nanocomposites because of better distribution of nanofillers in polymer matrix. Depending on the distribution of nanofiller, these polymer nanocomposites can be classified as intercalated nanocomposites, exfoliated nanocomposites, and partially exfoliated nanocomposites.[13,34] In case of intercalated nanocomposites, nanofillers (DS-LDH) are set on a regular basis and located parallel to each other. However, for the layer spacing greater than 9 nm, it may lead to the formation of exfoliated nanocomposites and usually show better results because of the homogeneous and disordered distribution of nanofiller in polymer matrix.[8] When some LDH layers are located parallel to each other in addition to some unevenly distributed layers throughout the polymer matrix, partially exfoliated nanocomposites are formed.

Polyurethane (PU) is a versatile polymeric material that can be adapted to meet the diversified demands of modern technologies, such as coating, foams, composites, thermoplastic elastomer and reaction molding plastics, fibers, etc.[23,34] It has a wide range of physical and chemical properties. It is biodegradable and also has high Young modulus together with very high elongation at break (EB). Therefore, it has high tear strength and abrasion resistance compared to other polymers. Its practical applications are unlimited in drug delivery, in the field of automobile industry, in coating, in cable-sheathing and as adhesives for textile, leather, paper, wood, and glass fibers. Various inorganic fillers have commonly been used in PU to reduce formulation cost and to increase its stiffness. However, the improvement in modulus for conventional PU nanocomposite is compromised by elastomeric properties.[36,37]

In this article, we report the synthesis of PU/Mg-Al LDH nanocomposites through solution intercalation method. To make uniform dispersion of LDH in polymer matrix, the pristine LDH is made organiphilic by intercalation of dodecyl sulfate (DS) anion in the interlayer and examine the effect of DS-LDH loading on PU. The nanocomposites have been characterized by X-raydiffraction (XRD), Fourier transform infrared (FTIR), scanning electron microscopy (SEM), transmission electron microscopy (TEM), and flame retardancy analysis. We have also investigated the mechanical properties and the thermal properties of PU/DS-LDH nanocomposites.

EXPERIMENTAL

Materials

PU, polyether type thermoplastic elastomer, received from Bayer (Desmopan-9385), Germany, is a thermoplastic elastomer with melt flow rate of 4 cc/10 min and density 1.12 g/cc. NaOH (S.D.Fine chemicals, Boisar), $Mg(NO_3)_2\cdot 6H_2O$, $Al(NO_3)_3\cdot 9H_2O$ (E.Merck, India), and sodium dodecyl sulfate (SRL Pvt., Mumbai, India) were used as received. Tetrahydrofuran (THF) was purchased from SRL, Mumbai, India, and was dried with 0.3 nm molecular sieves over night followed by refluxing with sodium metal and finally distilled under reduced pressure.

Preparation of organophilic LDH (DS-LDH)

DS-LDH was synthesized by standard coprecipitation and thermal crystallization method. Na_2CO_3 [2.65 g (0.025 mol)] and NaOH [8 g (0.2 mol)] were

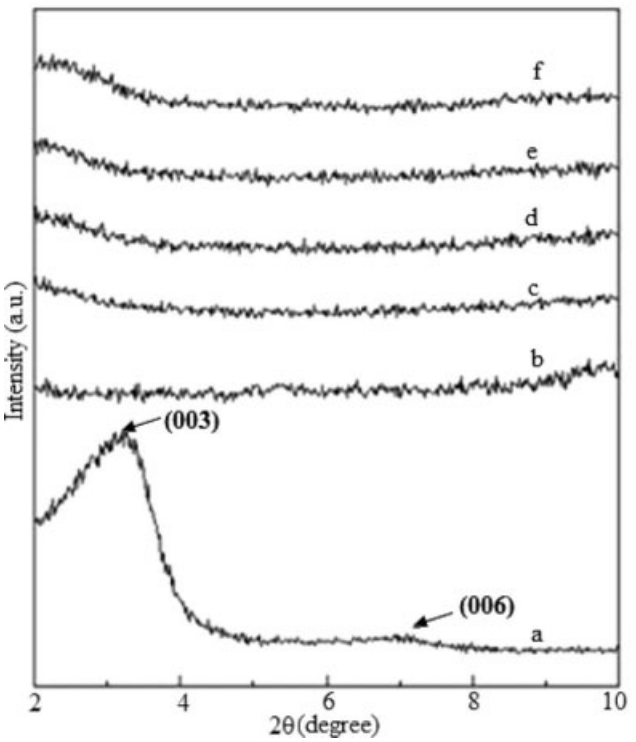

Figure 2 XRD spectra of (a) pure DS-LDH, (b) pure PU and its nanocomposites containing (c) 1 wt %, (d) 3 wt %, (e) 5 wt %, and (f) 8 wt % DS-LDH.

dissolved in 100 mL of deionized water at room temperature followed by the addition of 100 mL aqueous solution of $Mg(NO_3)_2{\cdot}6H_2O$ [19.65 g (0.075 mol)] and $Al(NO_3)_3{\cdot}9H_2O$ [9.25 g (0.025 mol)] under nitrogen atmosphere. The solution pH was adjusted to 10 ± 0.1 using 1*M* NaOH solution. After aging the resulting white precipitate at 70–75°C for 27 h, it was filtered, washed, and dried. The dried LDH was finally calcined at 500°C for 6 h and then suspended in a solution of 4 g of SDS dissolved in 200 mL of deionized water maintained at 70°C under stirring condition for 12 h followed by refluxing for 6 h at 100°C. The product finally filtered and dried under vacuum at 60°C for 3 days to yield a white powder DS-LDH.

Synthesis of DS-LDH/PU nanocomposites

The 1, 3, 5, and 8 wt % of DS-LDH were dispersed in 30 mL dry THF at 60°C in 100 mL round-bottom flask and stirred for about 6 h. In another 250 mL round-bottom flask, PU was dissolved in dry THF at the same temperature as before. Subsequently, the respective amounts of dispersed DS-LDH were added to the PU solution under stirring conditions at 60°C for 6 h followed by solution casting of the resulting composites on Teflon petridish for drying under ambient conditions. The composites were subsequently roll milled at room temperature and finally subjected to compression molding at 170°C for 4 min.

CHARACTERIZATION

XRD studies of Mg-Al LDH, DS-LDH, pure PU, and their nanocomposites were carried out at room temperature on a Rigaku Miniflex diffractometer (30 kV, 10 ma) using Cu Kα radiation (η = 0.15418 nm).The distribution of DS-LDHs in PU matrix was studied with transmission electron microscope (JEM JEOL 2100) with acceleration voltage of 200 kV. Fourier transform infrared spectrum was carried out using Perkin-Elmer (FTIR Spectrometer RXI) over the wave number range of 400–4000 cm^{-1}. The tensile test of neat PU and its nanocomposites were measured on a Zwick/Roell Z010 according to ASTM D-412 and were elongated at the strain rate of 200 mm/min at (25 ± 2)°C. For each data point, five specimens were tested for each sample to obtain a reliable average and standard deviation for tensile strength (TS) and EB. SEM of tensile fracture surface of the nanocomposites was carried out on JEOL (JSM-5800) scanning electron microscope with an acceleration voltage of 20 kV. Thermogravimetric analysis (TGA) of virgin PU and its corresponding nanocomposites with DS-LDH (~ 5.3 mg) were carried out on Redcroft 870 thermal analyzer, Perkin-Elmer from 50 to 650°C with a heating rate of 10°C/min under N_2 atmosphere. The flame retardancy test of all the samples were carried out by the measurement of limiting oxygen index (LOI) value using flammability tester (S.C. Dey Co., Kolkata) as per the standard ASTM D 2863-77.

RESULTS AND DISCUSSION

X-ray diffraction study

Figure 2 shows the XRD pattern in the range of 2θ = 2°–10° for DS-LDH, neat PU, and PU/DS-LDH nanocomposites. The interlayer distance of DS-LDH and the nanocomposites can be calculated from Bragg diffraction law. The basal spacing of Mg-Al LDH (pristine LDH) is 0.78 nm,[38] whereas DS-LDH shows a sharp peak at 2θ = 3.41°, analogous to d_{003} peak with an inter layer distance of 2.59 nm. According to our earlier work,[18,34] individual dodecyl sulfate chain length and LDH sheet thickness are 2.07 and 0.48 nm, respectively. Therefore, the increase in basal spacing (roughly 1.81 nm) is because of interaction of monolayer dodecyl sulfate molecules between the hydrotalcite sheets. But in case of MMT and organomodified MMT (modified by dodecyl ammonium chloride), the basal spacing are 1.19 and 1.58 nm, respectively.[3] This suggests that the organomodification of LDH by dodecyl

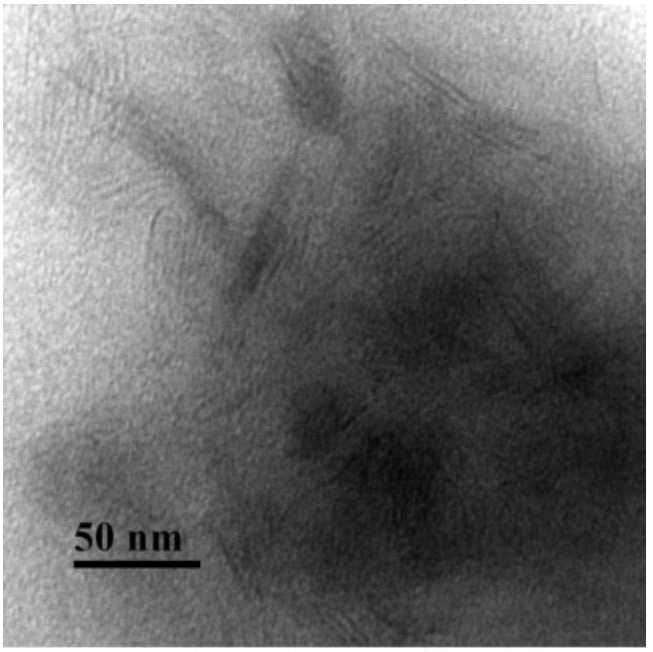

(a)

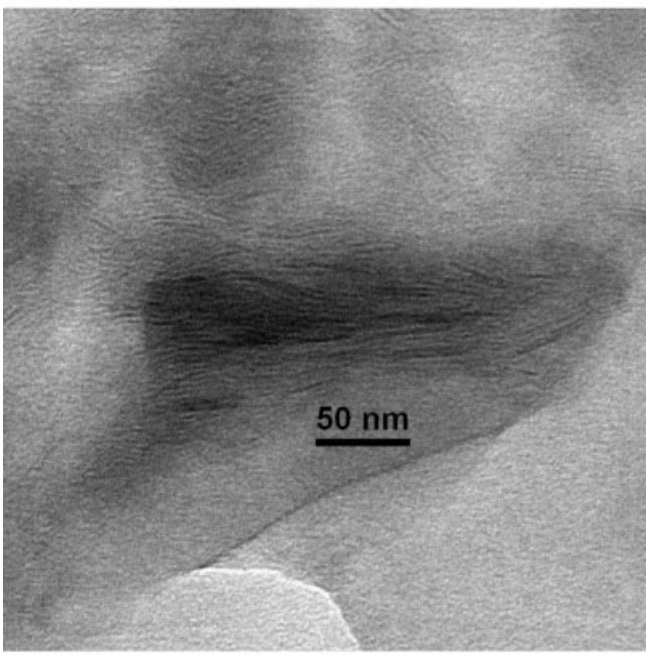

(b)

Figure 3 TEM images of (a) PU/DS-LDH (3 wt %) nanocomposite and (b) PU/DS-LDH (8 wt %) nanocomposite.

sulfate anions results in relatively more gallery height in comparision to the organomodifed MMT. In the case of PU/DS-LDH nanocomposites containing 1, 3, and 5 wt % of DS-LDH, the d_{003} and d_{006} peaks of DS-LDH are completely absent. On the contrary, a small hump is observed for the nanocomposites containing 8 wt % DS-LDH. This observation suggests that the organically modified Mg-Al LDH layers are partially or completely exfoliated and intercalated in PU matrix at lower filler (1, 3, and 5 wt %) and at higher filler (8 wt %) loading, respectively.[12–18] This is probably due to the loss of crystalline symmetry in the stacking direction of the hydroxide layers, lowering the number of hydroxide layers and also lot of insertion of polymer chain into the inter gallery space of DS-LDH.[39] XRD provides a partial picture about the distribution of nanofiller and disappearance of peak corresponding to *d*-spacing does not always confirm the exfoliated nanocomposites, beacause XRD is unable to detect regular stacking exceeding 8.8 nm.[8] Hence, a complete characterization of nanocomposite morphology requires microscopic investigation in these nanocomposites.[18]

Transmission electron microscopy analysis

Figure 3(a) shows the TEM image of PU/DS-LDH nanocomposite with 3 wt % of DS-LDH content. The dark lines represent the LDH layers, whereas the bright area represents PU matrix. The thickness and lateral size of the partially exfoliated LDH layers correspond to 4–6 nm and 30–50 nm, respectively. It is also evident from the TEM image that the LDH layers are dispersed partially in a disordered fashion in the polymer matrix. Although XRD does not give any concrete information about the dispersion of DS-LDH layers in PU matrix, the TEM image clearly shows molecular level distribution of the tiny clusters from the surface of DS-LDH layers in the form of partially exfoliated morphology. The TEM image of PU/DS-LDH nanocomposite with 8 wt % DS-LDH loading is shown in Figure 3(b) which confirms that the DS-LDH layers are intercalated in PU matrix. It demonstrates that some degree of structural regularity is maintained and the nanocomposites mainly comprises of parallel DS-LDH nanolayers with interlayer spacing of 5–6 nm which is greater than the spacing of DS-LDH.[34]

Fourier transform infrared analysis

Figure 4(a–c) shows the FTIR spectra of DS-LDH, pristine PU, and its nanocomposite containing 3 wt % DS-LDH. According to this, broad absorption bands at 3000 cm^{-1} and 3400–3600 cm^{-1} are observed in DS-LDH, due to —OH stretching frequency and hydrogen bonded —OH stretching of intercalated water molecules. The absorption at 1635 cm^{-1} is assigned to the bending vibration of interlayer water. The bands detected in the lower frequency region of the spectrum are deduced as the lattice vibration modes and can be attributed to M—O from 850 to 600 cm^{-1} and O—M—O at about 440 cm^{-1} (M = Mg, Al).[12,15] The peak at around 1382 cm^{-1} is due to the stretching mode of carbonate (CO_3^{2-}) anion.[34] The peaks at around 2851, 2920,

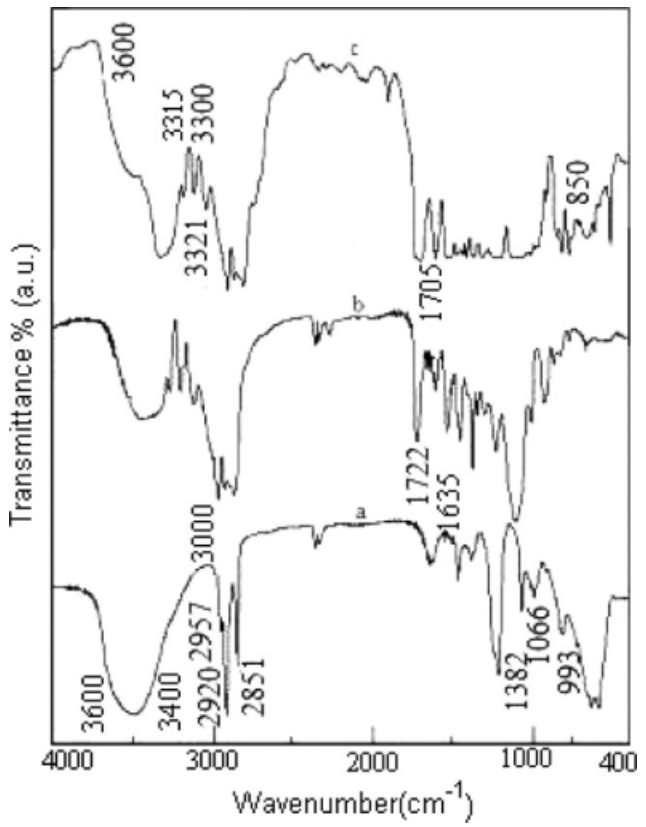

Figure 4 FTIR spectra of (a) DS-LDH, (b) PU, and (c) PU/DS-LDH nanocomposites (3 wt %).

2957 cm^{-1} and at 1218 and 1245 cm^{-1} correspond to the deformation vibration of —CH_3 and —CH_2 of long chain DS molecules and for the stretching vibration of sulfate in DS-LDH respectively.[15] The peaks at about 1066 and 993 cm^{-1} are due to the bending mode vibration of interlayer anions.[34] The IR spectra of PU shows characteristic stretching frequency at around 1722 and 3321 cm^{-1} corresponding to —C=O and —NH of the urethane bonds, respectively.[29,40] The presence of a broad peak is observed in the range of 3300 to 3600 cm^{-1} for PU nanocomposites. This may be due to the strong interaction through hydrogen bonding in between polar groups of PU and DS-LDH.[41] The shifting of IR peaks for the groups —NH (3315 cm^{-1}) and —C=O (1705 cm^{-1}) may be attributed to the hydrogen bond formation.[42] The lattice vibration bands appear in the region of 850–600 cm^{-1} in PU/DS-LDH nanocomposites[18] as shown in Figure 5. These peaks are absent in the case of neat PU, suggesting the existence of DS-LDH in pure PU.[34]

Mechanical properties

The effect of DS-LDH on the mechanical properties of PU/DS-LDH nanocomposites has been studied and the results are summarized in Figures 6 and 7.

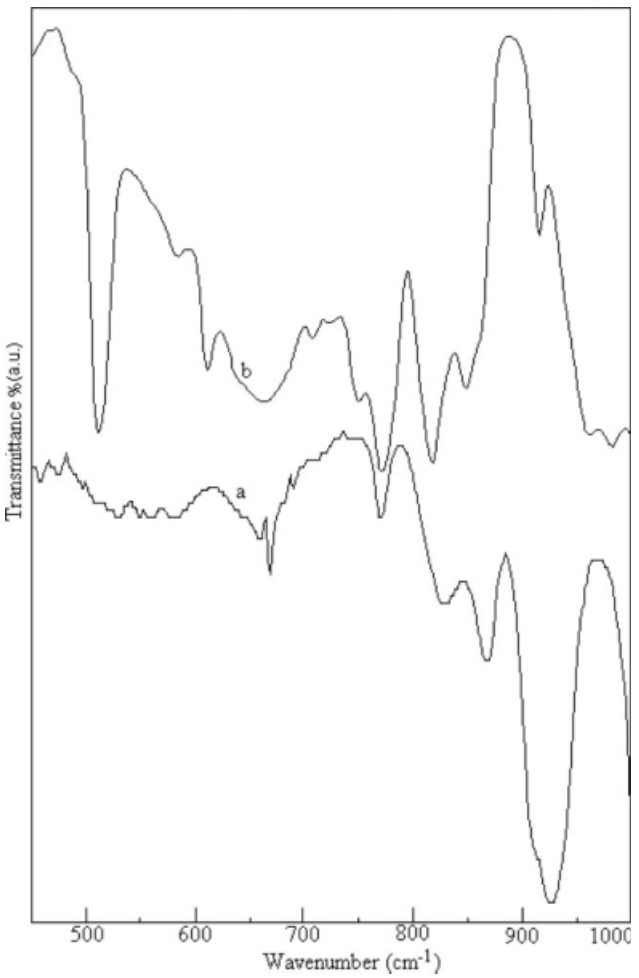

Figure 5 FTIR spectra of (a) PU and (b) PU/DS-LDH nanocomposites (3 wt %) between 450 and 1000 cm^{-1}.

Figure 6 shows stress–strain curves for neat PU and its DS-LDH nanocomposites. It is noted that the tensile modulus at different elongation percents

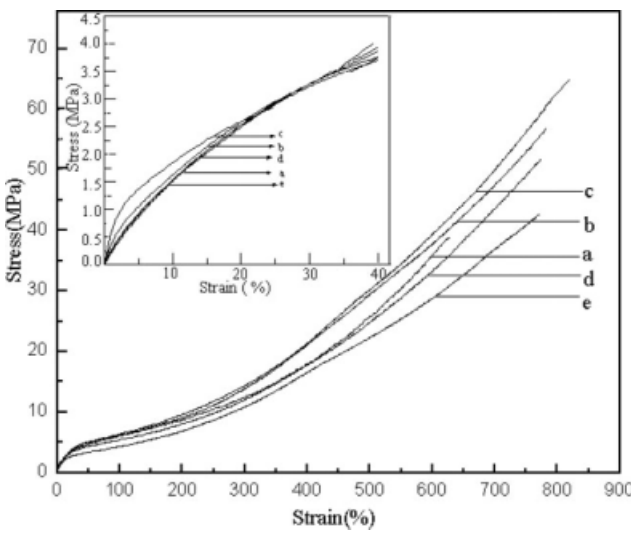

Figure 6 Stress–strain plot of (a) pure PU and its nanocomposites containing (b) 1 wt %, (c) 3 wt %, (d) 5 wt %, and (e) 8 wt % DS-LDH.

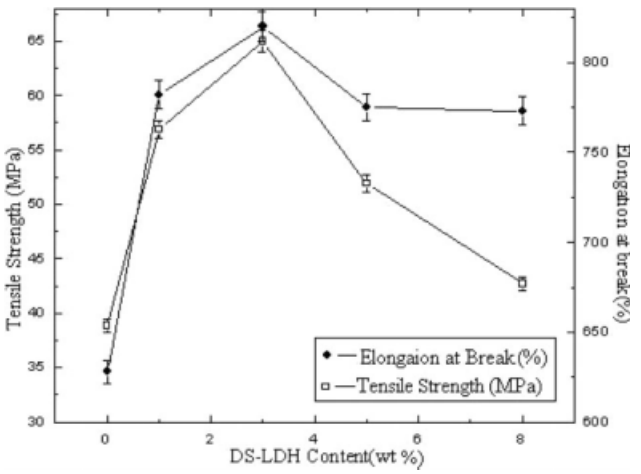

Figure 7 Variation of tensile strength (TS) and elongation at break (EB) of PU/DS-nanocomposites with DS-LDH contents.

increases up to 3 wt % DS-LDH loading in PU matrix and is probably due to the development of some shear zones when the nanocomposites are under stress and strain conditions.[34,43,44] The enhancement in tensile modulus may also be ascribed to the resistance applied by DS-LDH itself, as well as the orientation and high aspect ratio of the LDH platelets.[14,15] However, at lower elongation (below 50%), the tensile modulus is always higher for the nanocomposites except for 8 wt % DS-LDH loading (as shown in the inset of Fig. 6). This decrease in tensile modulus at higher DS-LDH content is attributed to the aggregation of DS-LDH layers where the cracking occurs easily resulting in low strain failure.[34,44]

It is seen from Figure 7 that the TS and EB for the nanocomposites containing 1, 3, 5, and 8 wt % DS-LDH are higher with respect to pristine PU. The TS is increased by 46, 67, 34, and 10% and EB is increased by 24, 27, 23, and 23% for PU nanocomposites containing 1, 3, 5, and 8 wt % DS-LDH. It shows that the maximum enhancement of TS and EB is observed for the nanocomposite with 3 wt % DS-LDH content. The increase in TS is due to the strong interfacial interaction between the hydroxyl group of DS-LDH and the polar urethane (—NHCOO) group of PU through the hydrogen bonding. It also appears that the partially exfoliated LDH layers transfer stress from LDH itself and directly enhance the stiffness of PU nanocomposites.[34] The enhancement in EB is due to the entanglement of the polymer chain and the synergistic effect of chain slippage and platlate orientation of DS-LDH layers.[39] The degree of improvement in TS and EB decreases beyond 3 wt % DS-LDH content as shown in Figure 7. This is probably due to the increasing tendency of aggregation of DS-LDH particles in the PU matrix. It appears that at higher DS-LDH content in PU, the aggregated layers cause a weak interaction between the DS-LDH layers and PU matrix. This is probably due to the inferior reinforcing effect of DS-LDH and formation of cracking through filler agglomerates in PU nanocomposites.[34,45]

Fracture surface morphology

Figure 8(a,b) displays SEM micrographs of the tensile fracture surface of pristine PU and its nanocomposites containing 3 wt % DS-LDH. The morphology of neat PU shows large smooth area. It indicates that the pure PU possesses weak resistance toward the crack propagation. On the contrary, the nanocomposite surface is rougher and the crack propagation is different. In the nanocomposites, inorganic nanoparticle initiates a secondary crack at the organic–inorganic interface and forms fracture steps before unification with the propagating primary crack.[46] Regarding tensile-mechanical data, it appears that

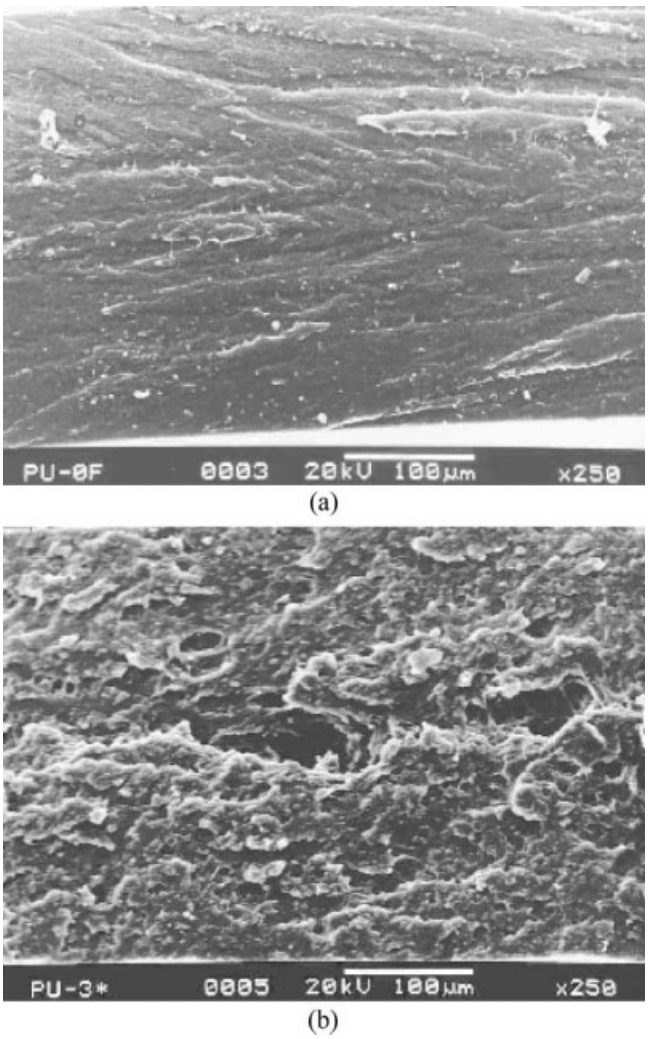

Figure 8 Fracture surface images of (a) neat PU (b) PU/DS-LDH (3 wt %) nanocomposite.

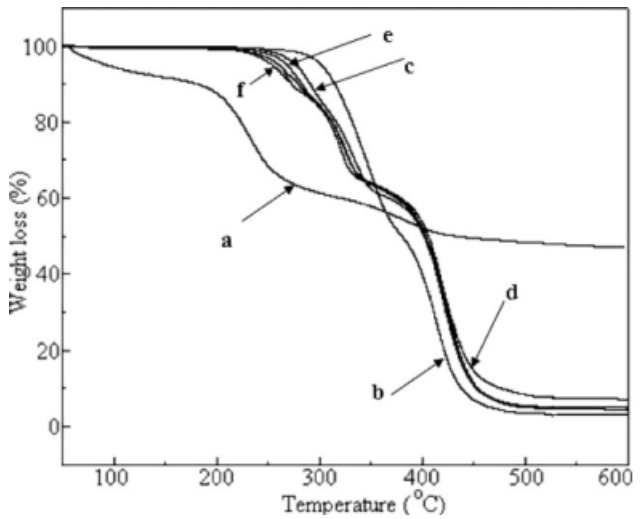

Figure 9 TGA curves of (a) DS-LDH (b) pure PU and its nanocomposites containing (c) 1 wt %, (d) 3 wt %, (e) 5 wt %, and (f) 8 wt % DS-LDH.

the rougher the fracture surface, the better are the mechanical properties of the respective nanocomposites. Hence, TS of nanocomposite increases compared to pristine PU. The possibility of formation of microvoids surrounding the DS-LDH particles forming the rough fracture surface impart the toughness, matrix shear yielding of the nanocomposites, is responsible for the enhancement of mechanical properties.[47,48]

Thermogravimetric analysis

Figure 9(a–f) shows the TGA of pure DS-LDH, pristine PU, and PU nanocomposites containing 1, 3, 5, and 8 wt % DS-LDH. According to this, the thermal degradation of neat PU and PU/DS-LDH nanocomposites generally passes through three stages.[49] The first stage of degradation of PU is mainly due to depolymerization which begins from 200 to 250°C due to the failure of urethane links releasing the polyol and isocyanate (monomers) used to synthesize PU chains. The monomers slowly volatilize during the continuous heating process. The complete volatilization of the resulting chain fragment is avoided by the dimerization of isocyanate to carbodiimides, which react with the alcohol groups to give relatively stable substituted ureas (second step from 378 to 446°C). The decomposition in the third step begins from 446 to 600°C, which is related to the decomposition of urea groups and corresponds to the high temperature degradation of these stabilized structures to yield small quantity of carbonaceous char.

TGA clearly shows that the weight loss in all the nanocomposites in the first step is due to the degradation of alkyl chains of organomodified LDH (DS-LDH).[16,18,19,34] In this, DS-LDH undergoes endothermic decomposition to liberate water and metal oxide. Such type of weight loss in the initial stage is extremely useful in promoting the charring process improving thereby the thermal stability of the nanocomposites.[16,50] The decomposition of DS-LDH is also shown in Figure 9(a) for its comparison and according to this, first decomposition starts at 169°C. The decomposition of dodecyl sulfate ions takes place at 210–250°C.[51] At 280–300°C, the loss of remaining carbonate and dehydroxylation of the host layers take place slowly. When 50% weight loss for PU and PU/DS-LDH nanocomposites containing 1, 3, 5, and 8 wt % DS-LDH are considered for the second stage in TGA, the decomposition takes place at 379, 401, 408, 405, and 403°C, respectively. This may be due to the presence of almost dispersed DS-LDH in PU matrix, which imparts barrier effect originated by anisotropic DS-LDH platelets that interrupts the release of volatile degradation products from these nanocomposites.[52] This clearly demonstrates that PU/DS-LDH nanocomposites have higher thermal stability than pristine PU. Similarly, when 84% weight loss is selected as point for comparison, the thermal decomposition temperatures of pure PU, and its nanocomposites with 1, 3, 5, and 8 wt % DS-LDH contents correspond to about 425, 438, 447, 439, and 441°C. It is also noted from Figure 9 that the third stage is relatively broader, where the weight loss ranges from 15 to 20% in the temperature range from 430 to 450°C. The composites displayed higher thermal resistance than pure PU. This may be attributed to further decomposition of the remaining fraction of polymers.[53] Such type of weight loss in the decomposition process promotes charring and enhances the fire safety of the nanocomposites.[16,18,19] The temperature corresponding to the maximum weight loss is highest for 3 wt % of DS-LDH/PU nanocomposite, possibly due to the

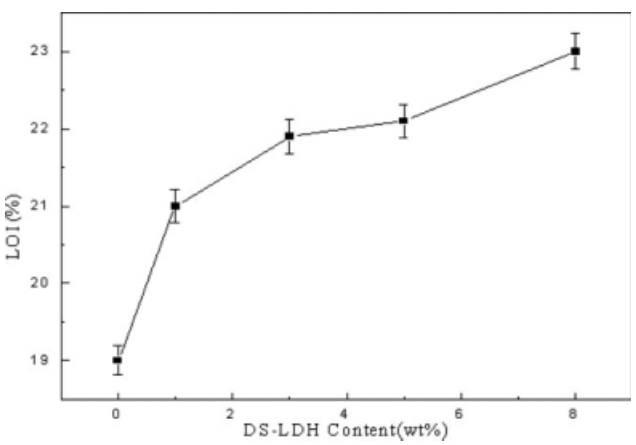

Figure 10 Influence of DS-LDH content on limiting oxygen index of PU/DS-LDH nanocomposites.

barrier effect of the mostly dispersed DS-LDH layers which inhibit the emission of small gaseous molecules during thermal decomposition. At higher DS-LDH filler loading, the thermal stability of the nanocomposites decreases due to the agglomeration of DS-LDH layer in PU matrix resulting in weak interaction between DS-LDH and PU matrix.[34]

Flame retardancy analysis

To evaluate the flame retardant properties of polymer materials, the LOI should be considered. Figure 10 shows the flame retardancy behavior of PU/DS-LDH nanocomposites. It is observed that the LOI values are improved with increasing the concentration of DS-LDH in PU. The LOI value is found to be $\sim$ 19% for neat PU and LOI values for the nanocomposites with 1, 3, 5, and 8 wt % DS-LDH content are increased to 21, 21.9, 22.1, and 23%, respectively. This type of behavior of LDH is likely to originate from the endothermic decompositions with the formation of water vapor and metal oxide residue which obstructs the burning process by reducing the oxygen supply to the bulk phase under the burning surface.[52] In addition, formation of char layer during burning also acts as a physical barrier against the propagation of downward flame along the LOI sample. The thickness of the char layer is observed to be very small on the burning surface at low LDH loading. As a result, this char is not able to provide efficient barrier effect and the samples burn quite easily at similar oxygen concentration as noted for neat PU. However, with increasing filler loading, both thickness of the char layer and the cooling effect from the endothermic decomposition of DS-LDH increases. Hence, self-sustained burning of the sample becomes more difficult with increase the LOI value with LDH loading.

CONCLUSIONS

Thermoplastic elastomer PU/DS-LDH nanocomposites have been successfully synthesized by solution blending of PU and DS-LDH. XRD and TEM analysis show that DS-LDH is exfoliated and distributed partially in the PU matrix. The mechanical properties of PU/DS-LDH nanocomposites are higher than that of pristine PU. The maximum tensile property is obtained from PU/DS-LDH nanocomposite containing 3 wt % DS-LDH ($\sim$ 67% higher) due to the partial exfoliation of DS-LDH in PU matrix. At higher filler loadings (5 and 8 wt %), tensile properties decrease due to the aggregation of DS-LDH layer which is again confirmed by TEM image of PU/DS-LDH (8 wt %) nanocomposite. TGA shows that the PU/DS-LDH nanocomposite containing 3 wt % DS-LDH increases by about 29°C signifying its higher thermal stability with respect to neat PU. Flame retardancy of the PU/DS-LDH nanocomposites increases from 19 to 23% than that of neat PU.

References

1. Alexandre, M.; Dubois, P. Mater Sci Eng R 2000, 28, 1.
2. Ray, S. S.; Okamoto, M. Prog Polym Sci 2003, 28, 1539.
3. Pramanik, M.; Srivastava, S. K.; Samantary, B. K.; Bhowmick, A. K. J Polym Sci Part B: Polym Phys 2002, 40, 2065.
4. Srivastava, S. K.; Pramanik, M.; Acharya, H. J Polym Sci Part B: Polym Phys 2006, 44, 471.
5. Maiti, M.; Bhowmick, A. K. Compos Sci Technol 2008, 68, 1.
6. Bandyopadhyay, A.; Maiti, M.; Bhowmick, A. K. Mater Sci Technol 2006, 22, 818.
7. Maiti, M.; Bhowmick, A. K. J Appl Polym Sci 2007, 105, 435.
8. Kornmann, X.; Lindberg, H.; Berglund, L. A. Polymer 2001, 42, 1303.
9. Liu, Z. H.; Yang, X. J.; Makita, Y.; Ooi, K. Chem Lett 2002, 31, 680.
10. Heising, J.; Kanatzidis, M. G. J Am Chem Soc 1999, 121, 638.
11. Nakato, T.; Furumi, Y.; Terao, N.; Okhura, T. J Mater Chem 2000, 10, 737.
12. Oriakhi, C.; Farr, I. V.; Lernal, M. M. Clays Clay Miner 1997, 45, 194.
13. Costa, F. R.; Abdel-Goad, M.; Wagenknechi, U.; Heinrich, G. Polymer 2005, 46, 4447.
14. Tseng, C. H.; Hsueh, H. B.; Chen, C. Y. Compos Sci Technol 2007, 67, 2350.
15. Du, L.; Qu, B.; Meng, Y.; Zhu, Q. Compos Sci Technol 2006, 66, 913.
16. Chen, W.; Feng, L.; Qu, B. Chem Mater 2004, 16, 368.
17. Pradhan, S.; Costa, F. R.; Wagenknecht, U.; Jehnichen, D.; Bhowmick, A. K.; Heinrich, G. Eur Polym J 2008, 44, 3122.
18. Acharya, H.; Srivastava, S. K.; Bhowmick, A. K. Compos Sci Technol 2007, 67, 2807.
19. Du, L.; Qu, B. J Mater Chem 2006, 16, 1549.
20. Cypes, S. H.; Saltzman, W. M.; Giannelis, E. P. J Control Release 2003, 90, 163.
21. Zhu, J.; Uhl, F. M.; Morgan, A. B.; Wilkie, C. A. Chem Mater 2001, 13, 49.
22. Gorrasia, G.; Tortoraa, M.; Vittoria, V.; Pollet, E.; Lepoittevin, B.; Alexandre, M. Polymer 2003, 44, 2271.
23. Szep, A.; Szabo, A.; Toth, N.; Anna, P.; Marosi, G. Polym Degrad Stab 2006, 91, 593.
24. Song, L.; Hu, Y.; Tang, Y.; Zhang, R.; Chen, Z.; Fan, W. Polym Degrad Stab 2005, 87, 111.
25. Karger-Kocsis, J. KGK 2006, 59, 537.
26. Finnigan, B.; Martin, D.; Halley, P.; Truss, R.; Campbell, K. Polymer 2004, 45, 2249.
27. Kumar, B.; Rana, S.; Singh, R. P. Exp Polym Lett 2007, 1, 748.
28. Hu, Y.; Song, L.; Xu, J. Colloid Polym Sci 2001, 279, 819.
29. Moon, S. Y.; Kim, J. K.; Nah, C.; Lee, Y. S. Eur Polym J 2004, 40, 1615.
30. Gianelli, W.; Camino, G.; Dintcheva, N. T.; Verso, S. L.; Mantia, F. P. L. Macromol Mater Eng 2004, 289, 238.
31. Leroux, F.; Besse, J. P. Chem Mater 2001, 13, 3507.
32. Li, F.; Zhang, L.; Evans, D. G.; Forano, C.; Duan, X. Thermochim Acta 2004, 424, 15.
33. Rives, V.; Kannan, S. J Mater Chem 2000, 10, 489.
34. Kuila, T.; Acharya, H.; Srivastava, S. K.; Bhowmick, A. K. J Appl Polym Sci 2007, 104, 1845.
35. Hsueh, H. B.; Chen, C. Y. Polymer 2003, 44, 1151.
36. Tien, Y. I.; Wei, K. H. Macromolecules 2001, 34, 9045.
37. Jeong, E. H.; Yang, J.; Hong, J. H.; Kim, T. G.; Kim, J. H.; Youk, J. H. Eur Polym J 2007, 43, 2286.
38. Chibwe, K.; Jones, W. Chem Commun 1989, 14, 926.

39. Kuila, T.; Acharya, H.; Srivastava, S. K.; Bhowmick, A. K. J Appl Polym Sci 2008, 108, 1329.
40. Pattanyak, A.; Jana, S. C. Polymer 2005, 46, 3275.
41. Ramaraj, B.; Jaisankar, S. N. Polym Plast Technol Eng 2008, 47, 733.
42. Yilgor, E.; Yurtsever, E.; Yilgor, I. Polymer 2002, 43, 6561.
43. Tang, C.; Xiang, L.; Su, J.; Wang, K.; Yang, C.; Zhang, Q.; Fu, Q. J Phys Chem B 2008, 112, 3876.
44. Kuila, T.; Srivastava, S. K.; Bhowmick, A. K.; Saxena, A. K. Compos Sci Technol 2008, 68, 3234.
45. Xiong, J.; Liu, Y.; Yang, X.; Wang, X. Polym Degrad Stab 2004, 86, 549.
46. Acharya, H.; Srivastava, S. K.; Bhowmick, A. K. Polym Eng Sci 2006, 46, 837.
47. Teh, P. L.; Mohd Ishak, Z. A.; Hashim, A. S.; Karger-Kocsis, J.; Ishiaku, U. S. Eur Polym J 2004, 40, 2513.
48. Costa, F. R.; Satapathy, B. K.; Wagenknecht, U.; Weidisch, R.; Heinrich, G. Eur Polym J 2006, 42, 2140.
49. Berta, M.; Lindsay, C.; Pans, G.; Camino, G. Polym Degrad Stab 2006, 91, 1179.
50. Chen, W.; Qu, B. Chem Mater 2003, 15, 3208.
51. Leroux, F.; Pagano, M. A.; Intissar, M.; Chauviere, S.; Rorano, C.; Besse, J. P. J Mater Chem 2001, 11, 105.
52. Costa, F. R.; Wagenknecht, U.; Heinrich, G. Polym Degrad Stab 2007, 92, 1813.
53. Rehab, A.; Salahuddin, N. Mater Sci Eng A 2005, 399, 368.